

INFLUENCE OF PORE SIZE DISTRIBUTION ON PENETRATION RESISTANCE BEHAVIOUR AND DRY DENSITY OF CLAY-LOAM SOIL

Patrik Prikner, Radka Kodesova

Czech University of Life Sciences in Prague
prikner@tf.czu.cz, kodesova@af.czu.cz

Abstract. A semi-empirical penetration resistance model is presented. The procedure utilizes a relationship based on the pore size distribution (in log-normal form) in terms of the change of soil dry density and gravimetric soil water content supporting correlations to penetration resistance per unit depth. Tests were performed using clay-loam as a standardized soil type for the soil water contents 14, 15, 17 and 19 %, respectively. Compacting levels 50, 75, 100 and 150 kPa were correlated to the changes in pore radius (using a log-normal pore size distribution model). The penetration resistance was measured below the centre of the load. The model was used to evaluate a uniformly precompacted soil profile and the compacting state at contact pressures of 300 kPa for the soil water content 17.5 % and 200 kPa for 19.5 % (corresponding to 75 and 85 % soil plastic limit) demonstrating correlations of 0.94 and 0.97, respectively, to the predetermined soil dry density.

Keywords: penetration resistance, pore size distribution, soil water content, soil dry density.

Introduction

In-situ measurements of soil compaction are based on different approaches (e.g., stress-strain transducers, gamma-ray, in-situ simulation, etc.). These in situ observations are typically calibrated/verified with basic core sampling techniques. In practice, extensive time and resources can be required for defining the soil state through these methods. Cone penetrometer or other types of direct soil state measurements can also be used for evaluation of the soil bulk density, such as the empirical relations based on the penetration techniques presented by Canarache [1]. Penetration resistance has been successfully demonstrated for specifying the soil physical properties in soil science, e.g., the degree of saturation, pore size distribution or soil strength etc. [2-4]. Empirical models have been introduced for relating the soil strength resistance and moisture content to changes of the bulk density. Ayers [5] developed empirical models for non-cohesive frictional soil types, while Hernanz [6] introduces models for the sandy loam soil type. In this study we introduce additional soil parameters beyond soil resistance and soil moisture to improve correlations to the soil state. Extending the research presented in [7], the model is introduced, based on the soil hydraulic properties. We utilize the relationships of pore-size distribution in log-normal form published by Kosugi [8] to improve the models relating the soil penetration resistance to the soil state. The main purposes of this paper are: 1) defining a relationship between the pore radius (corresponding to the mean of the pressure head natural logarithm obtained from fitting the soil-water retention using a log-normal distribution) and the penetration resistance and 2) defining a relationship between the soil dry density and the evaluated pore radius.

Materials and methods

The model has been initially defined around a single standard soil type obtained from the surface horizon in Chernozem. The texture of the soil is 27 % clay, 48 % silt and 25 % sand, and thus is specified as clay loam by both the Czech and USDA textural classification systems [9, 10]. Soil plastic limit (*SPL*) is 22 % gravimetric soil water content θ (*SWC*). Soil particles larger than 2 mm were removed. The relationships between the penetration resistance and the soil state were established with laboratory tests conducted with a soil container (usable volume 72 dm³) filled from the bottom to the top by even soil layers 5 cm high and each layer compacted by a round compacting plate.

The modelling in the soil container included three steps:

- filling combined with soil pre-compaction to produce a soil compaction characteristic;
- filling combined with modelling of uniform soil profile of the desired dry density;
- compaction state modelling.

The first step included sixteen compaction combinations, where eight soil layers were separately compacted using the mean contact pressure levels 50, 75, 100 and 150 kPa. $SWCs_{\theta}$ ($\text{cm}^3 \cdot \text{cm}^{-3}$) $\cdot 100$ % were evaluated in the range 14 ÷ 20 % with a tolerance $x \pm 0.5$ %. In the second modelling step, the soil

in the container was pre-compacted (eight layers 5 cm high) to achieve of a uniform soil profile in two variants; the first, as a simulation of natural field conditions for the soil water content $\theta_0' = 17.0^{\pm 0.5} \%$ (equal to 75 % soil plastic limit) with average soil dry density $\rho_{dl} = 1.330 \pm 0.015 \text{ g}\cdot\text{cm}^{-3}$; the second, the soil water content $\theta_0' = 19.5 \pm 0.5 \%$ (85 % soil plastic limit) with average soil dry density $\rho_{dl} = 1.420^{\pm 0.015} \text{ g}\cdot\text{cm}^{-3}$ represents the critical soil state [9]. The compaction state, top of the uniform pre-compacted soil column represents the ground surface, was loaded with a selected round pressure plate S_p with desired mean contact pressure to produce the modelling imprint; (more details see in [11]). The soil compaction in terms of dry density change along the soil column underneath this imprint produces the compaction function $\rho_d = f(z_p)$. It is presumed that the minimum modelling depth (height of the soil profile) is 26 cm as this allows a minimum of five samples to be taken along the compacted soil column with probe cylinders 3.4 cm high and of 6.3 cm bore, i.e. with volume 104 cm^3 .

Four strain gauges (Lukas Tenzo, the Czech Republic, type S-22, nominal load 0.5 kN, guaranteed accuracy $\pm 0.1 \%$) were used for defining the vertical resistance force. The penetration resistance PR_0 , values obtained in the centre of the soil column supporting a description of essential resistance behaviour according to ASAE S313.3 FEB04 standards [12], the cone angle 30° with the standard cone base area $S_{scb} = 1.29 \text{ cm}^2$, 1.283 cm diameter (Fig. 1a) with 0.953 cm diameter of the driving shaft 45 cm in length for hard soils were used (Fig. 1b,c). Stainless steel 416 material was used (AISI 416 standards) [13]. The rate of penetration was fixed at $3 \text{ cm}\cdot\text{sec}^{-1}$ using an optical sensor depth control system reading the force at 0.8 cm spacing (Fig. 1d). Penetration depth was 45 cm. The penetration resistance PR (MPa) is expressed as a ratio of acting pressure force F_p (kN) to the standard cone base area S_{scb} (cm^2).

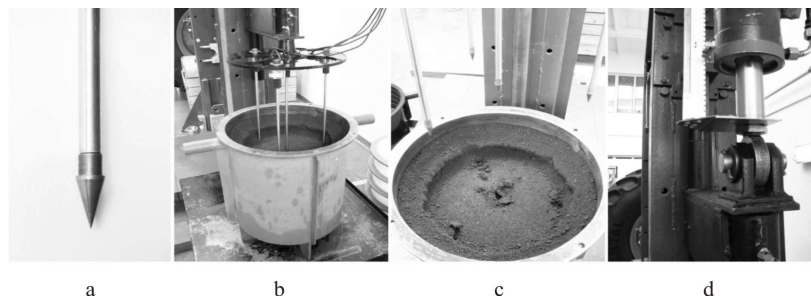


Fig. 1. **Equipment for penetration resistance measuring:** a – penetration cone ASAE S313.3; b – penetration test technique; c – situation after penetration resistance measurement; d – detail of optical sensor in depth control system – spacing 0.8 cm (range 0-45 cm)

The soil water retention curves (*SWR*) were examined in the laboratory on the undisturbed 100 cm^3 soil samples (soil core height of 5.1 cm and cross-sectional area of 19.60 cm^2). Data points of the soil water retention curve were evaluated using the final soil water content and water outflow. θ_r , θ_s , h_0 and σ_h parameters were obtained for soil parameters supporting the Kosugi's equation [8]:

$$\theta_e = \frac{\theta(h) - \theta_r}{\theta_s - \theta_r} = \frac{1}{2} \operatorname{erfc} \frac{\ln(h/h_0)}{\sqrt{2\sigma_h}} \quad h < 0 \quad (1)$$

$$\theta_e = \theta_s \quad h \geq 0,$$

- where θ_e – effective soil water content, $\text{cm}^3\cdot\text{cm}^{-3}$;
 θ – initial soil water content, $\text{cm}^3\cdot\text{cm}^{-3}$;
 θ_r – residual soil water content, $\text{cm}^3\cdot\text{cm}^{-3}$;
 θ_s – saturated soil water content, $\text{cm}^3\cdot\text{cm}^{-3}$;
 h – pressure head, cm;
 h_0 – pressure head in *SWR*, cm;
 σ_h – surface tension in log-normal pore-size distribution, Pa;

The equivalent pore radius r_0 (μm) was calculated assuming Laplace equation:

$$r_0 = \frac{2\sigma\cos\gamma}{\rho_w g h_0} \tag{2}$$

where σ – surface tension between the water and air, Pa;
 γ – contact angle of water curvature in soil pores, °;
 ρ_w – density of water, g·m⁻³;
 g – acceleration of gravity, m·s⁻².

The pore size – calibration function establishes a relationship between the soil pore radius distribution (derived from the log-normal distribution model) and the penetration resistance for specific water content (Fig. 2). The pressure head parameter (h_0) is derived from *SWR* characteristic and used for calculation of the pore radius r_0 in log-normal form. Pore size distribution in clay – loam, a soil type with higher aggregate stability, is directly correlated to the change of the compression state of the soil [14]. The pore size - calibration function is presented in the form $r_0' = f(PR_0, \theta_0')$ as an estimate of r_0' and used for calibration of the soil water content $\theta_0' \leftrightarrow \theta(h)$ from (1), thus the behaviour depends solely on PR_0 :

$$r_0' = 331 PR_0^{-1.172} \theta_0'^{-0.714} \tag{3}$$

$$R^2 = 91.67 \% \text{ (adjusted for } d.f.), F\text{-ratio} = 83.58, p < 0.001,$$

where r_0' – specific pore size in calibration form, μm;
 PR_0 – penetration resistance, MPa;
 θ_0' – calibration of soil water content, %.

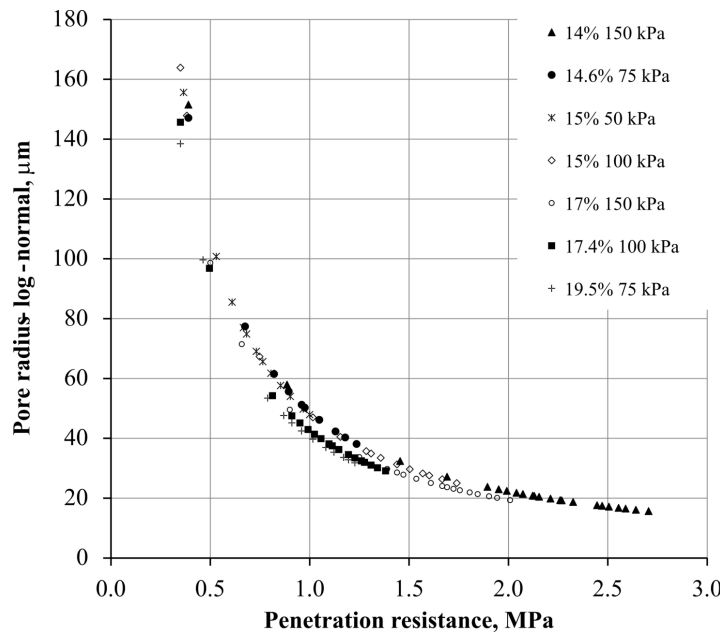


Fig. 2. Pore radius in log-normal form as penetration resistance calibration function

The soil compaction state as defined by the change in dry density uses penetration resistance as correlated to the pore radius size. The model is designed as follows; when the actual soil water content θ_0 is directly related to the calibration value θ_0' , eq.(3) can be applied for conversion of penetration resistance PR_0 for a soil of given r_0' . Soil dry density ρ_d (g·cm⁻³) as related to the specific pore radius r_0' in calibration form is modified to incorporate depth z_p in (4) using regression to establish the coefficients:

$$\rho_d = 1.299 r_0'^{-0.153} \theta_0'^{0.235} z_p^{-0.022} \tag{4}$$

$$R^2 = 93.84 \% \text{ (adjusted for } d.f.), F\text{-ratio} = 77.28, p < 0.001,$$

where ρ_d – soil dry density, g·cm⁻³;

r_0' – specific pore size in calibration form, μm ;
 θ_0 – actual soil water contents, $\text{cm}^3 \cdot \text{cm}^{-3}$;
 z_p – actual depth in soil profile, cm.

Results and discussion

Validation of the semi-empirical model was conducted using the observed penetration resistances. Behaviour of penetration resistance for compacted soils using the standard compacting pressure plate (contact area 531 cm^2) with mean contact pressure 300 kPa (load $\approx 1.6 \text{ Mg}$) is shown in Fig. 3. Figure 4 presents an example of assessment of soil dry density applying the semi-empirical model with input data of penetration resistance in regular depth intervals and *SWC*.

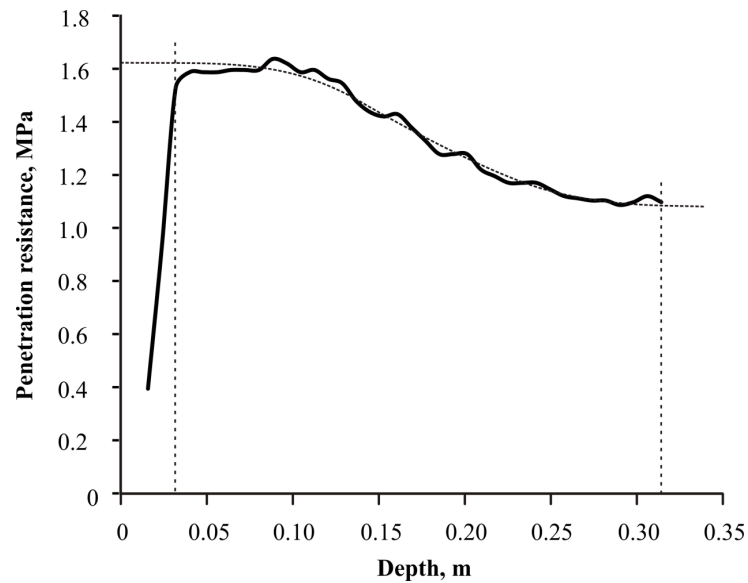


Fig. 3. Trend of penetration resistance in 300 kPa soil compaction state: $\rho_{d0} = 1.325 \text{ g} \cdot \text{cm}^{-3}$, *SWC* = 17.7 %, applied depth range from 3.2 to 31.2 cm

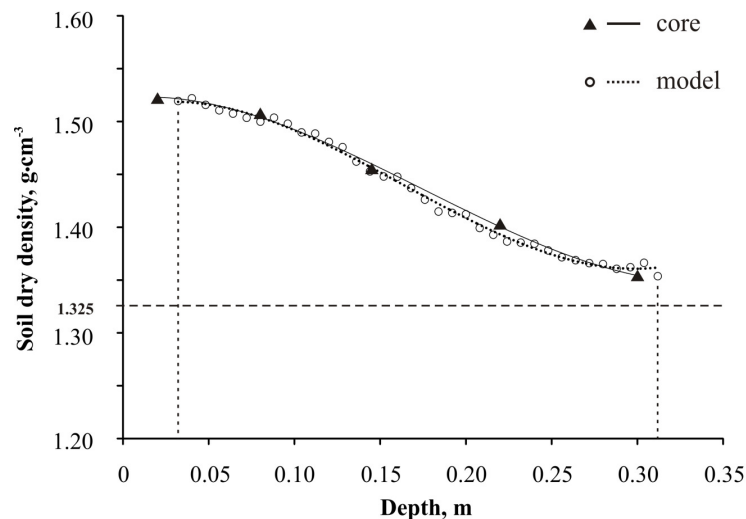


Fig. 4. Observed soil dry density behaviour under 300 kPa soil compaction state: $r = 0.97$, $\rho_{d0} = 1.325 \text{ g} \cdot \text{cm}^{-3}$, *SWC* = 17.7 %

The model was developed to predict the soil dry density using a standardized modelling technique. Penetration resistance is the primary input with a precise scanning in the tolerance value $\pm 0.5 \%$ measured in a depth optimal interval $0.5 \div 1.0 \text{ cm}$. Additional inputs include a soil water retention characteristic test, measured with a minimal number of two soil samples for each depth of interest. In comparison, the data obtained from all penetration tests confirm the estimated *PR* range for

clay content published by Canarache in [15]. SWR characteristic is implemented as a new procedure; thus the testing procedure desires to use the soil profile height 35 cm minimally for extraction at least of two soil samples in different depths. Figure 5 shows as an example a typical behaviour of SWR curves for four soil samples taken from uniformly *precompacted* soil profile where average $\rho_d = 1.325 \text{ g}\cdot\text{cm}^{-3}$ (P8 \rightarrow 8 cm and P22 \rightarrow 22 cm). In the soil profile *compacting* state under contact pressure 300 kPa (plate area 531 cm^2), the symbols C8 and C22 represent the behaviour of the SWR curves for two soil samples taken in the same depth positions, respectively.

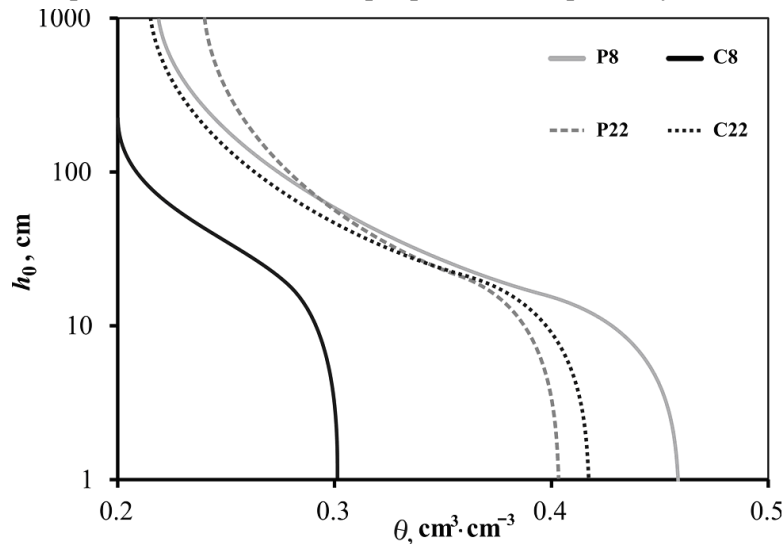


Fig. 5. Example of soil water retention curves:P8 and P22 (precompacted soil state) against C8 and C22 (300 kPa compaction state)in clay loam soil

The model technique is derived from eqs. (3) and (4), respectively. Fig. 6 illustrates the model pattern for the applied moisture conditions, where the depth z_p as an additional factor simply assigns the horizontal position of the plot area. The depth 2.5 cm states the operating level where the soil state is possible to be evaluated altogether competently. Further, the model presents consistent behaviour with Söhne's variation of porosity and compaction for different moisture levels published in [16].

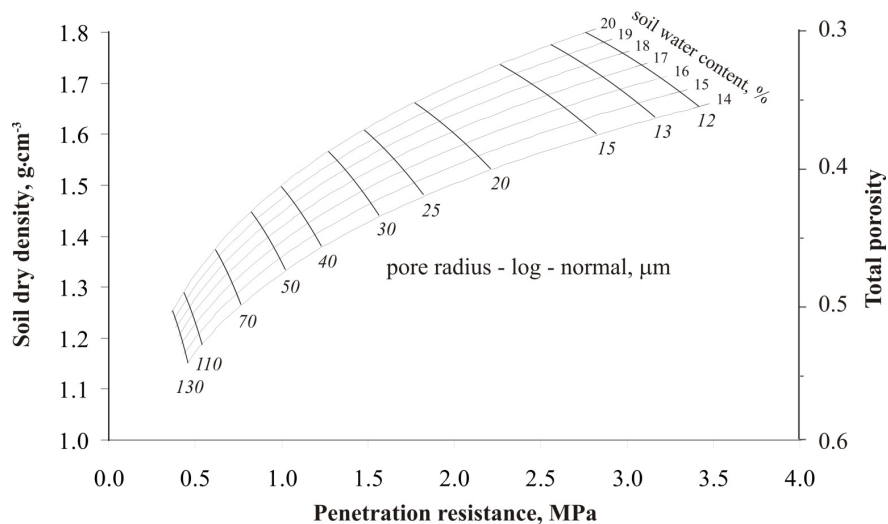


Fig. 6. Presentation of clay – loam soil pattern including total porosity verification scale (start depth 2.5 cm)

Conclusions

Penetration resistance in combination with the pore size distribution model was applied into a semi-empirical model for precise establishment of soil dry density in the modelled soil conditions. The model implemented on clay loam soil type includes estimation of the pore radius size as the

calibration value using the log-normal distribution model obtained from the soil retention characteristic for specific water contents up to 20 % representing 85 % soil plastic limit for clay-loam. The databank of conversion functions in terms of pore radius change describes penetration resistance behaviour in the range from 0.25 to 4 MPa under different water contents from 14 to 20 %, it can be established with accuracy 91.67 %. The principle of the pore size – conversion function and the measured penetration resistance in actual soil state, the calculation of soil dry density are proved with minimal accuracy 92 % $\approx (\pm 0.025 \text{ g}\cdot\text{cm}^{-3})$ under extreme compaction state 300 kPa. It is necessary to advise that the strictly uniform soil conditions have to be kept for observing of precise outputs, acceptable soil dry density corridor $\pm 0.015 \text{ g}\cdot\text{cm}^{-3}$. The semi-empirical model was developed for a standardized soil type clay-loam exclusively, thus the modelling pattern depends on a single soil texture response.

References

1. Canarache A. PENETR – a generalized semi-empirical model estimating soil resistance to penetration. *Soil Till. Res.*, vol. 16, 1990, pp. 51-70.
2. Dexter A.R., Czyż E.A., Gate O.P. A method for prediction of soil penetration resistance. *Soil Till. Res.*, vol. 93, 2007, pp. 412-419.
3. Horn R., Hartge K.H., Bachmann J., Kirkham M.B. Mechanical stresses in soils assessed from bulk density and penetration resistance data sets. *Soil Sci. Soc. Am. J.*, vol. 71, 2007, pp. 1455-1459.
4. Bachmann J., Contreras K., Hartge K.H., MacDonald R. Estimating soil stress distribution by using depth-dependent soil bulk density data. *J. Plant Nutr. Soil Sci.*, vol. 169, 2006, pp. 233-238.
5. Ayers P.D., Bowen H.D. Predicting soil density using cone penetration resistance and moisture profiles. *Trans. ASAE*, vol. 30, 1987, pp. 1331-1336.
6. Hernanz J.L., Peixoto H., Cerisola C., Sánchez-Girón V. An empirical model to predict soil bulk density profiles in field conditions using penetration resistance, moisture content and soil depth. *J. Terramech.*, vol. 37, 2000, pp. 167-184.
7. Prikner P. Penetration resistance – a suitable approach to evaluate the environmental risk of harmful soil compaction. Paper No. 052. In.: *Proceedings of the Joint 9th Asia-Pacific ISTVS Conference and Annual Meeting of Japanese Society for Terramechanics*, September 27-30, 2010, Sapporo, Japan.
8. Kosugi K. Lognormal distribution model for unsaturated soil hydraulic properties. *Water Resour. Res.*, vol. 32, 1996, pp. 2697-2703.
9. Lhotský J. Soil compaction and measures against it. *Study Inf. Plant Product.*, Prague: IAFI; 2000, No.7, (In Czech, abstract in English).
10. Clark, S.J. A proposed soil classification system for soil-vehicle and tillage mechanics. *J. Terramech.*, vol. 10, 1973, pp. 9-19.
11. Grečenko A., Prikner P. Tire rating based on soil compaction capacity. *J. Terramech.*, vol. 52, 2014, pp. 77-92.
12. ASAE Standards, ASAE S313.3 FEB04, Soil cone penetrometer, St. Joseph, MI: ASAE. 2004.
13. AISI standards, AISI PB 224 stainless steels, Steel Framing Alliance, Washington.
14. Kutílek M., Jendele L., Panayiotopoulos K.P. The influence of uniaxial compression upon pore size distribution in bi-modal soils. *Soil Till. Res.*, vol. 86, 2006, pp. 27-37.
15. Canarache A. Factors and indices regarding excessive compactness of agricultural soils. *Soil Till. Res.*, vol. 19, 1991, pp. 145-164.
16. Söhne W. Agricultural engineering and terramechanics. *J. Terramech.*, vol. 5, 1969, pp. 9-30.